

Quasiparticle band structures of β -HgS, HgSe, and HgTe

A. Svane,¹ N. E. Christensen,¹ M. Cardona,² A. N. Chantis,³ M. van Schilfgaarde,⁴ and T. Kotani⁵

¹*Department of Physics and Astronomy, Aarhus University, DK-8000 Aarhus C, Denmark*

²*Max-Planck-Institut für Festkörperforschung, Heisenbergstrasse 1, D-70569 Stuttgart, Germany*

³*American Physical Society, 1 Research Road, Ridge, New York 11961, USA*

⁴*School of Materials, Arizona State University, Tempe, Arizona 85287-6006, USA*

⁵*Department of Applied Physics and Mathematics, Tottori University, Tottori 680-8552, Japan*

(Received 8 June 2011; revised manuscript received 30 September 2011; published 10 November 2011; corrected 21 November 2011)

The electronic structures of mercury chalcogenides in the zinc-blende structure have been calculated within the LDA, GW (G_0W_0 , “one-shot”) and quasi-particle self-consistent GW (QSGW) approximations, including spin-orbit (SO) coupling. The slight tendency to overestimation of band gaps by QSGW is avoided by using a *hybrid* scheme (20% LDA and 80% QSGW). The details of the GW bands near the top of the valence bands differ significantly from the predictions obtained by calculations within the LDA. The results obtained by G_0W_0 depend strongly on the starting wave functions and are thus quite different from those obtained from QSGW. Within QSGW, HgS is found to be a semiconductor, with a Γ_6 s -like conduction-band minimum state above the valence top Γ_7 and Γ_8 (“negative” SO splitting). HgSe and HgTe have negative gaps (inverted band structures), but for HgTe the Γ_7 state is below Γ_6 due to the large Te SO splitting, in contrast to HgSe where Γ_6 is below Γ_7 . There appears to be significant differences, in particular for HgSe and HgS, between the ordering of the band-edge states as obtained from experiments and theory.

DOI: [10.1103/PhysRevB.84.205205](https://doi.org/10.1103/PhysRevB.84.205205)

PACS number(s): 71.20.Nr, 78.55.Et, 71.30.+h

I. INTRODUCTION

For many years it has been believed that the cubic mercury chalcogenides HgX ($X = \text{S, Se, and Te}$) belong to the group of materials that have so-called “inverted band structures,” “zero-,” or “negative-” gap materials similar to that of gray tin (α -Sn).¹ In the inverted band structures the, for many semiconductors, “usual” s -like conduction-band minimum state (Γ_6) has moved below the conventional Γ_8 valence-band maximum. From magnetoreflexion experiments Groves *et al.*² concluded that HgTe has this inverted band structure, and that $E_0 = -0.29$ eV. Here, the gap is defined as the difference between the Γ_6 and Γ_8 levels, $E_0 \equiv E(\Gamma_6) - E(\Gamma_8)$. The spin-orbit splitting, $\Delta_0 \equiv E(\Gamma_8) - E(\Gamma_7)$, was found to be larger than $-E_0$, i.e., the Γ_7 state would lie below Γ_6 . The photoemission experiment by Orłowski *et al.*³ demonstrated the inverted band structure of HgTe and suggested that the gap is $E_0 = -0.29$ eV at 40 K and -0.32 eV at 300 K. The SO splitting was found to be $\Delta_0 = 0.91$ eV.

Photoelectron spectroscopic experiments carried out by Gawlik *et al.*⁴ on n -type HgSe indicated that this material should have a positive band gap of 0.42 eV. Later experiments, including the photoemission study by Janowitz *et al.*⁵ could not verify this, and it was concluded that HgSe is a semimetal. However, the experimental resolution was not high enough to allow a firm determination of the Γ_6 , Γ_7 , Γ_8 level sequence. In fact HgSe is probably the HgX compound that has been most studied experimentally; see Refs. 6–8 in addition to those mentioned above. The paper by Einfeldt *et al.*⁸ includes further a compilation of a large amount of experimental results that show that there seems to be the consensus that E_0 is close to -0.2 eV and $\Delta_0 \approx 0.4$ eV.

Band-structure calculations within the local-density approximation (LDA) have also indicated that the bands are inverted. For HgS, LDA predicts that Γ_6 is below Γ_8 but Γ_7 is above Γ_8 by an amount that is sufficient to create a small

positive gap; see the discussion and Figs. 1 and 2 in Ref. 9. This is a result of the *negative* contribution to the spin-orbit (SO) splitting from the Hg- $5d$ states, which is larger in magnitude than the positive SO term from the S - p states. This is somewhat similar to the situation in CuCl.^{10,11}

The LDA band structures suffer from the so-called LDA band-gap error, causing the gaps in semiconductors to be severely underestimated. In order to circumvent this problem Rohlffing and Louie¹² calculated the band structure of HgSe within the GW (G : Green’s function; W : screened Coulomb interaction) scheme,¹³ and they found that Γ_6 is 0.51 eV below Γ_8 and Γ_7 0.30 eV below Γ_8 . This calculation uses the LDA wave functions, i.e., it is a “one shot” (G_0W_0) calculation. The LDA calculations by Fleszar and Hanke¹⁴ yielded negative E_0 gaps for all three mercury chalcogenides, whereas their GW (also G_0W_0) predicted a positive E_0 gap for HgS and negative for the selenide and the telluride. All their calculations gave negative values of Δ_0 for HgS, but positive for HgSe and HgTe. The same ordering of the levels at the Γ point was obtained for all three compounds by Moon and Wei who performed¹⁵ LDA calculations but included *transferable* gap-correcting external potentials as described in Ref. 16. For HgS there appear to be significant differences between theory and experiments. All the GW calculations by Fleszar and Hanke¹⁴ and the gap-corrected LDA calculations¹⁵ predict the gap to be positive, in contrast to what was concluded from some experiments.^{17,18} Very recently Sakuma *et al.*¹⁹ published GW calculations where the SO coupling was included directly in the calculation of G and W (i.e., not included as a formal perturbation as in Ref. 14 and in our work). They found that SO produces non-negligible modifications of, in particular, G . Their approach is still G_0W_0 . They found that E_0 in HgS is negative, -0.02 eV, but very small in magnitude.

Thus although the electronic structures of HgX ($X = \text{S, Se, Te}$) have been discussed by several researchers we feel

that there still are issues which need to be clarified. We shall attempt to do this here by presenting results of calculations within the QSGW approximation,^{20–22} and it will be argued that the results obtained by a “hybrid QSGW” scheme²³ (20% LDA and 80% QSGW) can be considered to be most reliable. It should be noted that we treat SO coupling as a perturbation, i.e., a somewhat cruder approximation than used in Ref. 19. However, we shall argue that effects of going beyond G_0W_0 , i.e., iterating as in QSGW, have a larger influence on the band structure. In addition, there may be other reasons for examining the details of the mercury chalcogenides. One apparent reason is that they, or alloys of them, may be three-dimensional (3D) topological insulators or quantum spin Hall insulators.^{24–26} Especially, the present study is interesting in connection to the recent prediction that β -HgS is a 3D topological insulator that, unlike any other known topological insulator, has a highly anisotropic Dirac cone and, consequently, quasi-one-dimensional topological surface states.²⁷

II. LDA AND QSGW BAND STRUCTURES

As mentioned in the Introduction we performed calculations within the LDA as well as the QSGW approximations.^{20–22} In both cases the basis sets are obtained in the linear muffin-tin orbital (LMTO)²⁸ formalism in the full potential implementation of Ref. 29. The QSGW calculations follow the lines described earlier, for example, for PbX ($X = S, Se, Te$).³⁰ Specifically, two sets of LMTO functions were used, of $spdf$ and spd character, with tails expanded to a cutoff of $\ell_{\max} = 6$. Additional floating orbitals²⁹ of spd character were included on interstitial sites, and local orbitals²⁹ were included to describe the chalcogen high-lying s , p , and d states, as well as the Hg high-lying p and d states. These extensions of the basis set ensure an accurate description of the conduction bands and their contribution to the screening of the interaction, which is particularly important for GW calculations. All scalar relativistic effects are included in the definition of the basis set, however, spin-orbit coupling (in the $\mathbf{L} \cdot \mathbf{S}$ approximation) is added only after quasiparticle self-consistency.

The LDA is not well suited for accurate calculations of band gaps in semiconductors, which is the reason why we apply the QSGW scheme. The band gaps obtained by this method agree much better with experimental data. In particular, for narrow-gap systems, where the screening is sensitive to the structure and magnitude of the gap,³¹ a self-consistent treatment in the band-structure calculation, as implemented in the QSGW approximation,^{20–22} is important. However, there is a systematic tendency to overestimating the band gaps; see, for example, Fig. 1 in Ref. 21 and Fig. 4 in Ref. 32. It has been shown²³ that the application of a *hybrid* approximation where the QSGW self-energy is reduced by a factor 0.80 leads to very good agreement with experimental band gaps. This was also found for the lead chalcogenides,³⁰ as well as for nitride semiconductors.³²

The overestimate of band gaps in calculations using the full QSGW approach was discussed (also) in Ref. 33, where the method was used for copper aluminate. The effect is large for wide-gap materials, i.e., including oxides, and it was ascribed to the omission of vertex corrections. These were estimated by

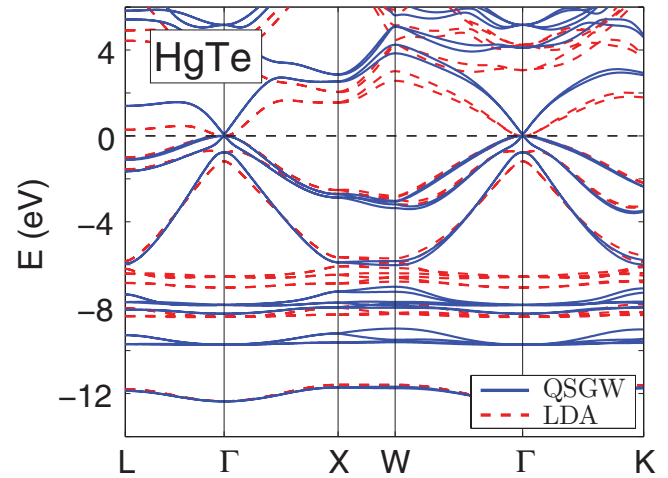


FIG. 1. (Color online) The band structure of HgTe as calculated within the LDA (dashed, red curves) and QSGW (blue, full-line curves) approximations. The zero of energy is at the valence-band maximum.

solving³⁴ the Bethe-Salpeter equation (BSE), which showed that for CuAlO_2 the BSE calculations reduce the apparent gap by an amount that is close to the amount by which the gap is overestimated by QSGW. Further, for several other semiconductors it was found that the gap reductions required to bring the QSGW gaps in agreement with experiments are very close to the electron-hole correlation-induced gap reductions (Δ_{e-h}) as calculated by Shishkin *et al.*³⁵

Before discussing the details of the gap-edge states, we show in Fig. 1 overall band structures of HgTe as obtained by LDA and QSGW, both with inclusion of SO coupling. The reference energy, $E = 0$, has in both cases been chosen to be that of the Γ_8 state. The dashed, red, and rather flat LDA bands around -6.5 eV and -8.2 eV are the SO-split semicore Hg $5d$ bands. As is usually found³³ the QSGW shifts the d bands toward lower energies with respect to the valence-band top. In HgTe this downshift amounts to ≈ 1.2 eV, the blue full-line curves around -7.7 eV and -9.5 eV, respectively. The semicore d states hybridize with the states at the top of the valence band, and their spectral position is therefore an important parameter influencing the details of these states, including their SO splitting. The GW thus reduces this influence as compared to LDA.

It follows from Figs. 1 and 2 that the LDA and QSGW bands near the valence-band maximum ($E = 0$) differ significantly. LDA predicts HgTe to be an inverted-gap material with Γ_6 lying 1.20 eV below Γ_8 and Γ_7 0.78 eV below Γ_8 . The full QSGW calculation places Γ_6 slightly above Γ_8 , whereas Γ_7 is close to the Γ_7 energy in the LDA bands, i.e., essentially the same SO splitting. The QSGW thus would predict HgTe to be a “normal” small-gap semiconductor. However, for HgTe both the LDA and QSGW predictions are wrong. The LDA result is incorrect due to the usual “LDA-gap error,” and the QSGW result is wrong due to the systematic overestimation^{21,32} of the band gaps.

Figures 2(b) and 2(c) illustrate the differences between the full and hybrid QSGW calculations of the band structure of HgTe. Figure 2(b) is the band structure of a normal

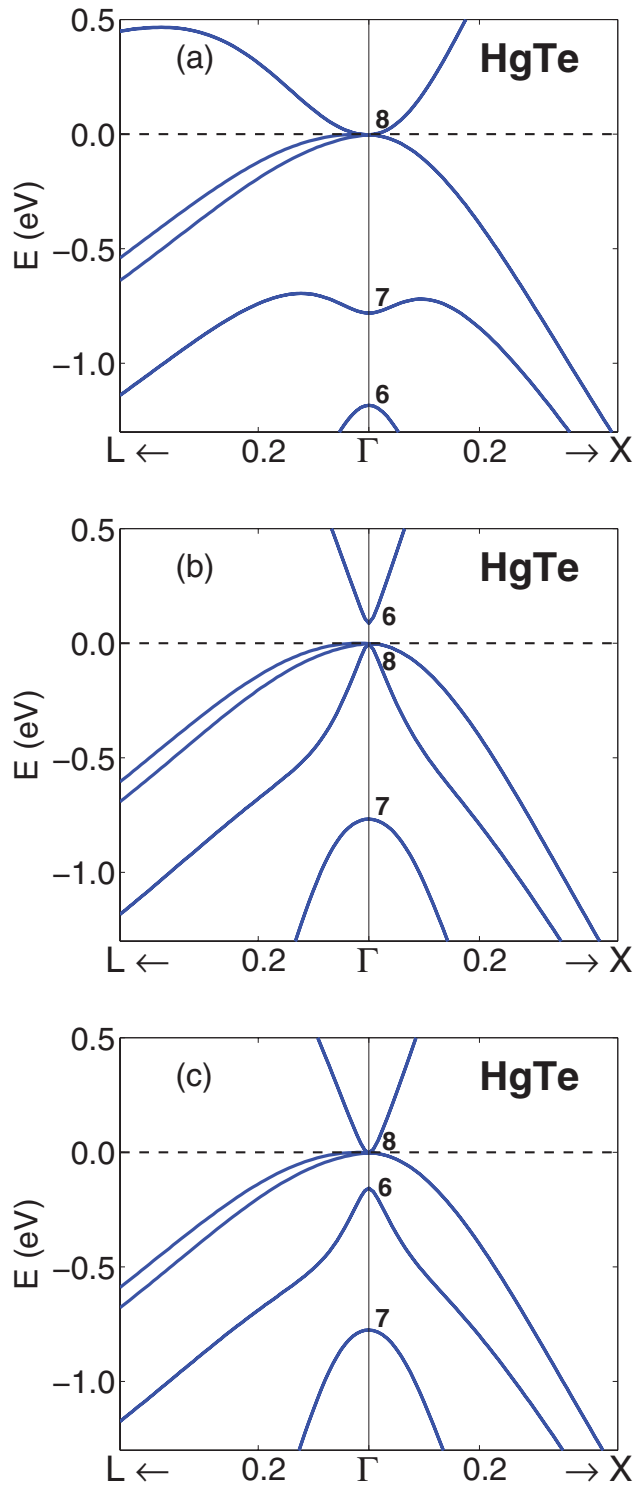


FIG. 2. (Color online) Band structure of HgTe near the Γ point as calculated by (a) the LDA approximation, (b) the full QSGW approach, (c) the *hybrid* QSGW approach. The unit along the x axis is $2\pi/a$, with $a = 6.47 \text{ \AA}$.

semiconductor with a small, 0.09 eV, gap, whereas the bands of Fig. 2(c) have the “inverted” structure, $E_0 = -0.18 \text{ eV}$, $\Delta_0 = 0.80 \text{ eV}$. We consider the level ordering in Fig. 2(c) to be the correct one, since it agrees with the angular resolved photoemission measurements by Orlowski *et al.*³

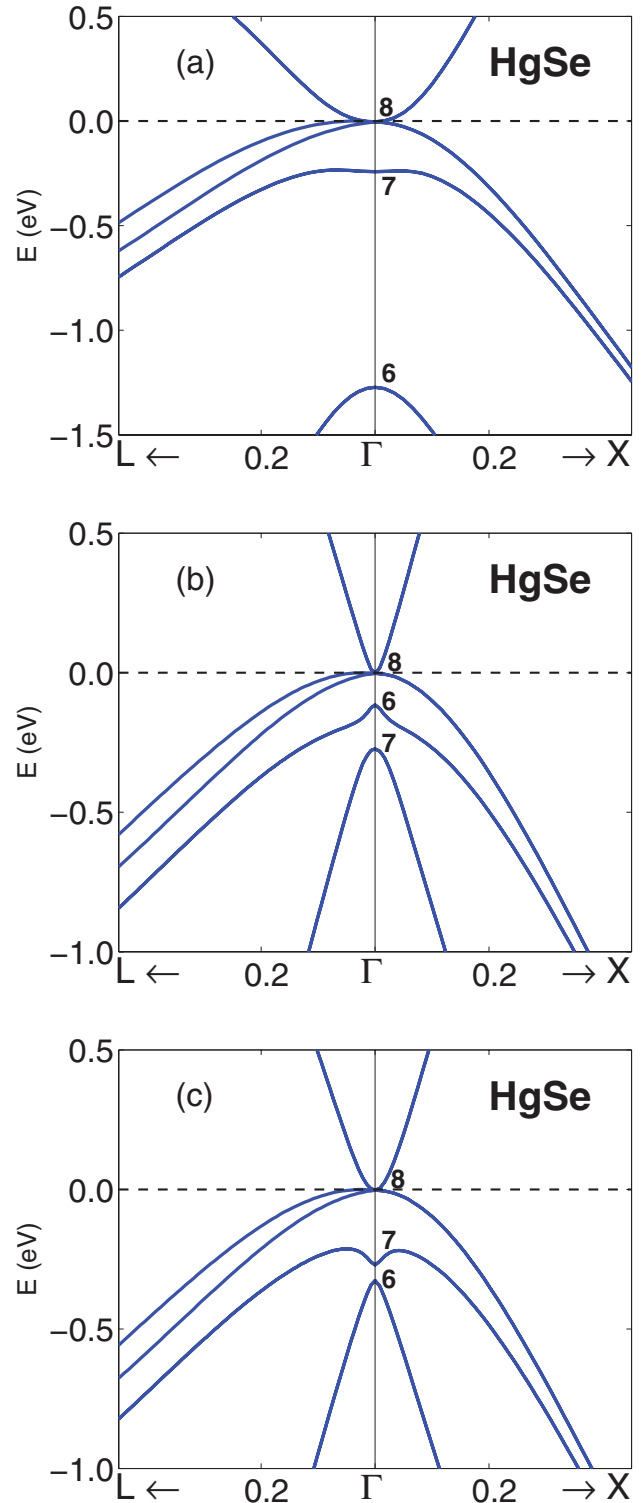


FIG. 3. (Color online) Band structure of HgSe near the Γ point as calculated (a) within the LDA, (b) within the QSGW approximation, and (c) with the *hybrid* QSGW approach. The unit along the x axis is $2\pi/a$, with $a = 6.08 \text{ \AA}$. Note that the energy scale in (a) differs from those in (b) and (c).

For HgSe the LDA predicts what appears to be the correct level ordering in the upper valence-band regime, with a negative E_0 and a positive Δ_0 as can be seen in Fig. 3(a).

But, due to the LDA gap error, the Γ_6 state is lying far too low relative to the Γ_8 state. On the other hand, the full QSGW moves the Γ_6 state to a much higher energy, now above the Γ_7 level, as shown in Fig. 3(b). The hybrid QSGW, Fig. 3(c), agrees considerably better with Ref. 12 and with experiments; see discussion in Ref. 12.

The mercury sulfide HgS may be considered to be the most intriguing of the three materials as far as the band structure is concerned. Experiments do not provide a unanimous picture; the experimental band gap ranges from -0.5 to $+0.5$ eV,³⁶ which is probably related to the difficulty of obtaining pure HgS samples so the extraction of the band-gap value has only been indirect so far. Within the LDA, the bands are in a sense *doubly inverted*. The LDA predicts, Fig. 4(a), a semiconducting nature. A small indirect gap, ≈ 0.05 eV exists [The valence-band maximum is not shown in the figure. It is found displaced from the Γ point, in the $(1,1,0)$ direction.] The bottom of the conduction band is not Γ_6 , but Γ_7 . This is the result of the negative SO splitting in HgS. The contribution to the SO interaction from the S- p states is smaller than the contribution coming from the interaction with the (semicore) Hg- $5d$ states. But the bands are also inverted in the more common sense: Γ_6 is below Γ_8 . The QSGW yields a quite different picture, Fig. 4(b). Again, HgS is predicted to be a semiconductor, now normal in the sense that the conduction-band minimum is the Γ_6 state. The minimum band gap is direct, but the state at the valence-band maximum is of Γ_7 character due to the ‘‘SO inversion’’ mentioned above.³⁷

Since we know that the full QSGW overestimates the (positive) Γ_6 - Γ_8 difference, we again consider the hybrid QSGW approach to provide the qualitatively and quantitatively best description of the band structure for these materials. Figure 4(c) shows the hybrid QSGW bands in the gap region of HgS. The level ordering is the same as obtained with the full QSGW, but the band gap (Γ_6 - Γ_7) is smaller, $E_g = 0.31$ eV and $E_0 = 0.37$ eV. The SO splitting is $\Delta_0 = -0.07$ eV.

Zallen and Slade assumed¹⁸ that the inverted-band structure model for gray tin¹ also applies to HgS, and on the basis of this, the analysis of their optical measurements of the plasma edge led them to the conclusion that E_0 should be -0.15 eV. However, our QSGW and hybrid QSGW do not support the fundamental assumption in Ref. 18 of the α -Sn model for HgS. As mentioned in the Introduction, Dybko *et al.*¹⁷ concluded from their Shubnikov-de Haas experiments that E_0 in HgS should be negative, and they quoted the value -0.11 eV (inverted gap). However, their Eq. (4), which is used in the fitting process, contains only the square of E_0 , and therefore information about the sign cannot be extracted. The *magnitude*, 0.11 eV, is significantly lower than our value of $E_g = 0.31$ eV, though. Dybko *et al.*¹⁷ also quote values of the ‘‘conduction electron mass,’’ in units of the free-electron mass (m_e), ranging from 0.039 to 0.070, depending on the doping. We calculated the effective electron mass in our hybrid QSGW approach and found it to be $0.031m_e$ at the Γ_6 conduction-band minimum. Further, it increases rapidly as the wave vector is shifted away from the Γ point, as can be seen from Fig. 5. Already 20 meV above the conduction-band minimum its value has increased to $0.04m_e$. The observed masses will then depend sensitively on doping. The mass $0.07m_e$ deduced from the plasma frequency¹⁸ then also may

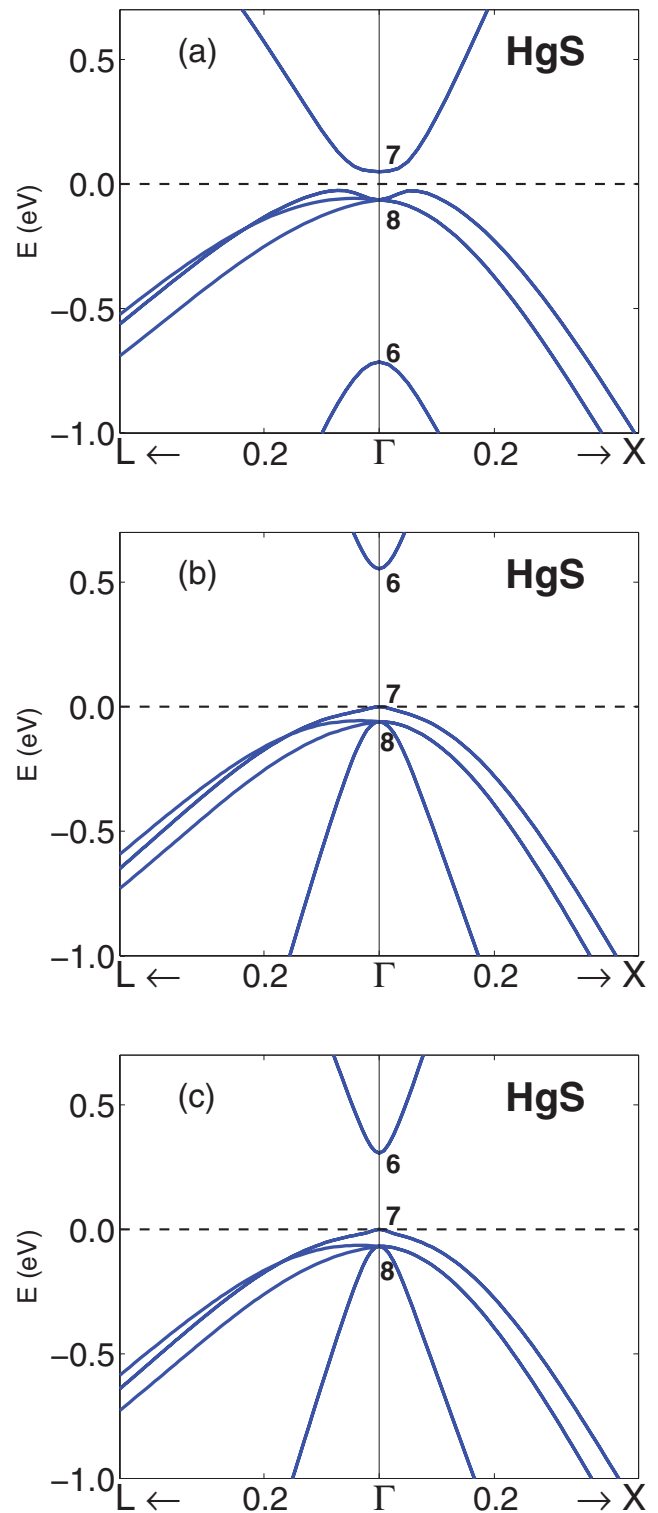


FIG. 4. (Color online) Band structure of HgS near the Γ point as calculated (a) within the LDA, (b) within the QSGW approximation, and (c) with the *hybrid QSGW* approach. $E = 0$ corresponds to the valence-band maximum, which in case (a) is found displaced off the Γ point, in the direction toward the K point. The unit along the x axis is $2\pi/a$, with $a = 5.84$ Å.

be consistent with our results. We believe that the reason why the band gaps in the experimental works of Refs. 17 and 18

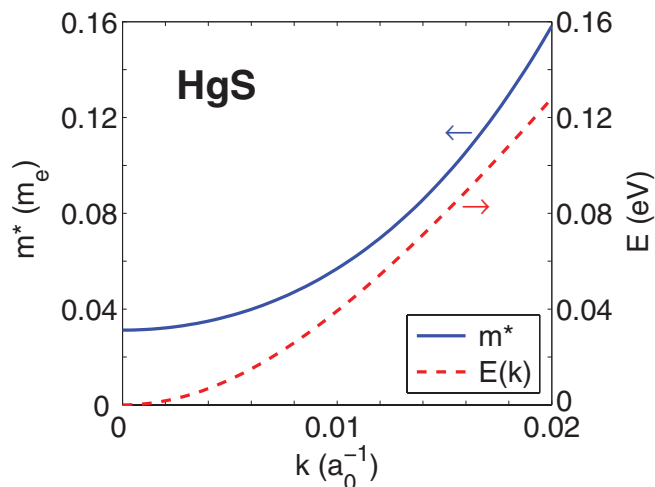


FIG. 5. (Color online) The lowest conduction band and the effective (“curvature”) mass of HgS near the Γ point as calculated by the *hybrid QSGW* approach (a_0 is the Bohr radius).

were quoted as being negative is that, at the time when these experiments were carried out, it was assumed to be “well established” that HgS should be a “negative-gap material.” Thus we do not question the quality of the experiments themselves.

Table I gives the values of the Γ_6 - Γ_8 energy difference (E_0) and the spin-orbit splitting (Δ_0) derived from our LDA, G_0W_0 , QSGW and hybrid-QSGW calculations together with LDA and GW (G_0W_0) results of Refs. 14 and 19 and some experimental results.

Our hybrid QSGW results agree reasonably well with the GW calculations of Ref. 14, presumably in principle closest to their $G'W'$ because this includes updating of the eigenvalues. However, for HgS and HgSe they disagree with the quoted results obtained from experiments. In all our calculations, LDA and QSGW, as well as in those of Ref. 14, it is found for each of the three compounds that the Δ_0 values are almost the same

TABLE I. Energy “gap,” $E_0 = E(\Gamma_6) - E(\Gamma_8)$, and spin-orbit splitting, $\Delta_0 = E(\Gamma_8) - E(\Gamma_7)$ in eV, calculated in the present work with the LDA, the one-shot G_0W_0 , the QSGW, and the hybrid QSGW (h -QSGW) approximations. Results of previous works are (a) LDA and $G'W'$ calculations from Ref. 14; (b) LDA and GW results from Ref. 19. The experimental data (c) are representative values from Ref. 8.

	HgS		HgSe		HgTe	
	E_0	Δ_0	E_0	Δ_0	E_0	Δ_0
LDA (present)	-0.63	-0.11	-1.18	0.24	-1.20	0.78
G_0W_0 (present)	0.08	-0.11	-0.45	0.24	-0.34	0.78
QSGW (present)	0.61	-0.06	-0.11	0.27	0.09	0.77
h -QSGW (present)	0.37	-0.07	-0.32	0.27	-0.18	0.80
LDA (a)	-0.62	-0.12	-1.23	0.23	-1.17	0.80
GW ($G'W'$) (a)	0.12	-0.13	-0.40	0.23	-0.48	0.80
LDA (b)	-0.66	-0.12	-1.27	0.23	-1.20	0.78
GW (b)	-0.02	-0.19	-0.58	0.32	-0.60	0.91
Expt.: (c)	-0.11		-0.20	0.45	-0.30	1.08

irrespective of which calculational scheme is used. This may seem surprising because the admixture of Hg-5d character into the valence-band maximum (VBM) states affects the SO splitting. Apparently, the downshift of the Hg-5d states caused by the GW relative to the LDA is so small, \approx one-tenth of the energy difference between the VBM and the Hg-5d states, that it does not affect the spin-orbit splitting markedly. The LDA calculation by Delin and Klüner³⁸ gave Δ_0 values that are very similar to those given in the upper part of the table. The SO splittings obtained by Sakuma *et al.*¹⁹ from their G_0W_0 are somewhat larger in magnitude due to their inclusion of the SO coupling in the GW calculation.

Considering the values of E_0 the table shows that iterating beyond G_0W_0 as in QSGW and hybrid QSGW has a strong influence. Thus E_0 increases by 0.53, 0.34, and 0.43 eV in HgS, HgSe, and HgTe, respectively, from the G_0W_0 approximation to full self-consistent QSGW. On the other hand, the Δ_0 parameter is only weakly influenced by the quasiparticle self-consistency. As mentioned earlier, the full QSGW has the tendency to overestimate the gaps, and the hybrid QSGW has proven to be a useful *ad hoc* correction for this as demonstrated earlier for many different materials. The increase in E_0 from the G_0W_0 approximation to the h -QSGW approximations is 0.29, 0.13, and 0.16 eV in HgS, HgSe, and HgTe, respectively.

III. SUMMARY AND CONCLUSIONS

The calculations described in the previous section have shown that the band structures for the mercury chalcogenides as calculated within the LDA and QSGW approximations differ significantly with respect to the ordering of the levels in the band-edge regimes as well as values of the characteristic gaps. The result as obtained by the hybrid QSGW approach shows that HgS is a semiconductor with an s -like Γ_6 conduction-band minimum state, but with the valence-band top being the Γ_7 split-off state, i.e., the SO splitting is inverted due to hybridization with the Hg-5d states. Thus this band structure is different from the model used in Ref. 27 to predict the presence of topologically protected edge states in β -HgS. Both HgSe and HgTe have inverted band structures with Γ_6 lying below Γ_8 . In HgSe Γ_7 is between the Γ_6 and Γ_8 levels, whereas the Te SO coupling in HgTe is so strong that Γ_7 falls below Γ_6 . All LDA calculations fail in describing these band details. This is not a surprise. But for HgTe the full and hybrid QSGW also predict different level orderings. We agree with Sakuma *et al.*¹⁹ that the effect of including the SO coupling in the calculation of G is important. We add it to the noninteracting QSGW Hamiltonian only after the self-consistent potential has been generated. But, on the other hand, we have shown that for HgX, the one-shot GW , G_0W_0 , inherits too much of the LDA gap error, and the iterations in the QSGW approach are essential (see also Ref. 26). Based on our experience with the applications of the QSGW approach to several other semiconductors we trust that the hybrid QSGW approximation gives the best quasiparticle energies. Still, the present calculations do not include prediction of spectral positions of exciton peaks, which may appear in the gaps observed in experimental absorption spectra. Calculations including these require further

treatment,³⁹ but this is not an issue for the present work. Based on the consistency between level orderings obtained in quasiparticle calculations of Refs. 12, 14, 15, and, apart from the marginal difference in the relative position in the Γ_6 level in HgS between Ref. 19 and the present work, we suggest that it might be worthwhile to re-evaluate the analyses of the experimental data, in particular those for HgS and HgSe. We are, however, aware that in particular the interpretation of the magnetoabsorption experiments, such as those by Dobrowolska *et al.*⁷, seems to rest on a rather firm foundation: the selection rules derived by Guldner *et al.*^{40,41} But these rules rely on a rather simple $\mathbf{k}\cdot\mathbf{p}$ s - p interaction band model, and it cannot be excluded that application of more

realistic band structures including interactions with many other states could have important effects.

ACKNOWLEDGMENTS

We thank R. Sakuma for sending us a preprint of Ref. 19 prior to publication. This work was supported by the Danish Agency for Science Technology and Innovation, Grant No. 09-072836. The calculations were carried out at the Centre for Scientific Computing in Aarhus, financed by the Danish Centre for Scientific Computing and the Faculty of Science, Aarhus University. M.v.S. was supported by NSF Grant No. QMHP-0802216.

-
- ¹S. H. Groves and W. Paul, *Phys. Rev. Lett.* **11**, 194 (1963).
²S. H. Groves, R. N. Brown, and C. R. Pidgeon, *Phys. Rev.* **161**, 779 (1967).
³N. Orłowski, J. Augustin, Z. Golacki, C. Janowitz, and R. Manzke, *Phys. Rev. B* **61**, R5058 (2000).
⁴K.-U. Gawlik, L. Kipp, M. Skibowski, N. Orłowski, and R. Manzke, *Phys. Rev. Lett.* **78**, 3165 (1997).
⁵C. Janowitz, N. Orłowski, R. Manzke, and Z. Golacki, *J. Alloys Compd.* **328**, 84 (2001).
⁶D. G. Seiler, R. R. Galazka, and W. M. Becker, *Phys. Rev. B* **3**, 4274 (1971).
⁷M. Dobrowolska, W. Dobrowolski, and A. Mycielski, *Solid State Commun.* **34**, 441 (1980).
⁸S. Einfeldt, F. Goschenhofer, C. R. Becker, and G. Landwehr, *Phys. Rev. B* **51**, 4915 (1995).
⁹M. Cardona, R. K. Kremer, R. Lauck, G. Siegle, A. Muñoz, and A. H. Romero, *Phys. Rev. B* **80**, 195204 (2009).
¹⁰M. Cardona, *Phys. Rev.* **129**, 1068 (1963).
¹¹A. Blacha, M. Cardona, N. E. Christensen, S. Ves, and H. Overhof, *Solid State Commun.* **43**, 183 (1982).
¹²M. Röhlfing and S. G. Louie, *Phys. Rev. B* **57**, R9392 (1998).
¹³L. Hedin and S. Lundqvist, in *Solid State Physics*, edited by H. Ehrenreich, F. Seitz, and D. Turnbull (Academic, New York, 1969), Vol. 23, p. 1.
¹⁴A. Fleszar and W. Hanke, *Phys. Rev. B* **71**, 045207 (2005).
¹⁵C.-Y. Moon and S.-H. Wei, *Phys. Rev. B* **74**, 045205 (2006).
¹⁶N. E. Christensen, *Phys. Rev. B* **30**, 5753 (1984).
¹⁷K. Dybko, W. Szuszkiewicz, E. Dynowska, W. Paszkowicz, and B. Witkowska, *Physica B* **256**, 629 (1998).
¹⁸R. Zallen and M. Slade, *Solid State Commun.* **8**, 1291 (1970).
¹⁹R. Sakuma, C. Friedrich, T. Miyake, S. Blügel, and F. Aryasetiawan, *Phys. Rev. B* **84**, 085144 (2011).
²⁰S. V. Faleev, M. van Schilfhaarde, and T. Kotani, *Phys. Rev. Lett.* **93**, 126406 (2004).
²¹M. van Schilfhaarde, T. Kotani, and S. V. Faleev, *Phys. Rev. Lett.* **96**, 226402 (2006).
²²T. Kotani, M. van Schilfhaarde, and S. V. Faleev, *Phys. Rev. B* **76**, 165106 (2007).
²³A. N. Chantis, M. van Schilfhaarde, and T. Kotani, *Phys. Rev. Lett.* **96**, 086405 (2006).
²⁴B. A. Bernevig, T. L. Hughes, and S. C. Zhang, *Science* **314**, 1757 (2006).
²⁵M. König, S. Wiedmann, C. Brüne, A. Roth, H. Buhmann, L. Molenkamp, X.-L. Qi, and S.-C. Zhang, *Science* **318**, 766 (2007).
²⁶J. Vidal, X. Zhang, L. Yu, J.-W. Luo, and A. Zunger, *Phys. Rev. B* **84**, 041109(R) (2011).
²⁷F. Viot, R. Hayn, M. Richter, and J. van den Brink, *Phys. Rev. Lett.* **106**, 236806 (2011).
²⁸O. K. Andersen, *Phys. Rev. B* **12**, 3060 (1975).
²⁹M. Methfessel, M. van Schilfhaarde, and R. A. Casali, *Lecture Notes in Physics* (Springer-Verlag, Berlin, 2000), Vol. 535, p. 114.
³⁰A. Svane, N. E. Christensen, M. Cardona, A. N. Chantis, M. van Schilfhaarde, and T. Kotani, *Phys. Rev. B* **81**, 245120 (2010).
³¹J. Vidal, S. Botti, P. Olsson, J.-F. Guillemoles, and L. Reining, *Phys. Rev. Lett.* **104**, 056401 (2010).
³²A. Svane, N. E. Christensen, I. Gorczyca, M. van Schilfhaarde, A. N. Chantis, and T. Kotani, *Phys. Rev. B* **82**, 115102 (2010).
³³N. E. Christensen, A. Svane, R. Laskowski, B. Palanivel, P. Modak, A. N. Chantis, M. van Schilfhaarde, and T. Kotani, *Phys. Rev. B* **81**, 045203 (2010).
³⁴R. Laskowski, N. E. Christensen, P. Blaha, and B. Palanivel, *Phys. Rev. B* **79**, 165209 (2009).
³⁵M. Shishkin, M. Marsman, and G. Kresse, *Phys. Rev. Lett.* **99**, 246403 (2007).
³⁶*Semiconductors Basic Data*, edited by O. Madelung (Springer-Verlag, Berlin, 2003).
³⁷See also *Note added in proof* in Ref. 9.
³⁸A. Delin and T. Klüner, *Phys. Rev. B* **66**, 035117 (2002).
³⁹R. Laskowski and N. E. Christensen, *Phys. Rev. B* **73**, 045201 (2006).
⁴⁰Y. Guldner, G. Rigaux, A. Mycielski, and Y. Couder, *Phys. Status Solidi B* **81**, 615 (1977).
⁴¹Y. Guldner, G. Rigaux, A. Mycielski, and Y. Couder, *Phys. Status Solidi B* **82**, 149 (1977).